



Get Clarity On Generics

Cost-Effective CT & MRI Contrast Agents



**FRESENIUS
KABI**

[WATCH VIDEO](#)

AJNR

Thalamic Massa Intermedia in Children with and without Midline Brain Malformations

M.T. Whitehead and N. Najim

AJNR Am J Neuroradiol 2020, 41 (4) 729-735

doi: <https://doi.org/10.3174/ajnr.A6446>

<http://www.ajnr.org/content/41/4/729>

This information is current as
of August 31, 2025.

Thalamic Massa Intermedia in Children with and without Midline Brain Malformations

M.T. Whitehead and N. Najim



ABSTRACT

BACKGROUND AND PURPOSE: The massa intermedia is a normal midline transventricular thalamic connection. Massa intermedia aberrations are common in schizophrenia, Chiari II malformation, X-linked hydrocephalus, Cornelia de Lange syndrome, and diencephalic-mesencephalic junction dysplasia, among others. We have noticed that massa intermedia abnormalities often accompany other midline malformations. The massa intermedia has never been formally evaluated in a group of exclusively pediatric patients, to our knowledge. We sought to compare and contrast the prevalence, size, and location of the massa intermedia in pediatric patients with and without congenital midline brain abnormalities.

MATERIALS AND METHODS: Successive 3T brain MR imaging examinations from pediatric patients with and without midline malformations were procured from the imaging data base at a pediatric hospital. Massa intermedia presence, size, morphology, and position were determined using 3D-T1WI with 1-mm isotropic resolution. The brain commissures, septum pellucidum, hypothalamus, hippocampus, vermis, and brain stem were evaluated to determine whether alterations were related to or predictive of massa intermedia abnormalities.

RESULTS: The massa intermedia was more frequently absent, dysmorphic, and/or displaced in patients with additional midline abnormalities than in those without. The massa intermedia was absent in 40% of patients with midline malformations versus 12% of patients with normal findings ($P < .001$). Massa intermedia absence, surface area, and morphology were predictable by various attributes and alterations of the commissures, hippocampus, hypothalamus, vermis, brain stem, and third ventricle.

CONCLUSIONS: Most pediatric patients have a thalamic massa intermedia centered in the anterior/superior third ventricle. Massa intermedia abnormalities are commonly associated with other midline malformations. Normal-variant massa intermedia absence is a diagnosis of exclusion.

ABBREVIATION: MI = massa intermedia

The massa intermedia (MI) is a normal midline transventricular thalamic link that develops around 13–17 weeks' gestational age.^{1–3} It is not considered a commissure because no reciprocal interhemispheric connections have been found within it in humans. Nonetheless, its cytoarchitecture suggests that it is functionally active.⁴ The MI comprises neurons and neuropil with circularly oriented fibers postulated to represent neurosphere correlates (neuronal and glial progenitors).^{4,5} Stria

medullaris fibers that modulate motivation and mood may cross through the MI as suggested by DTI tractography.⁶ In a separate DTI study, Damle et al⁵ showed that MI size correlates with anterior thalamic radiation integrity and mediates the relationship between age and attention in healthy female subjects.

Animal studies have also enhanced our understanding of MI anatomy and potential functions. Widespread frontal, perirhinal/pericruciate, and limbic axonal MI crossings have been documented histologically in monkeys, rats, and cats.⁷ Crossing nigro-caudate and caudo-caudate connections have also been identified.⁸ A rhesus monkey study demonstrated loss of the normal crossed tactile placing response in stroke-induced monkeys following concurrent transection of the corpus callosum and MI but not in stroke-induced monkeys after callosotomy alone, suggesting that the paralytic effect of cortical damage may be dampened with an intact MI and accentuated without it.⁹

Received October 21, 2019; accepted after revision January 22, 2020.

From the Department of Radiology (M.T.W., N.N.), Children's National Hospital, Washington, DC; and The George Washington University Hospital (M.T.W.), Washington, DC.

Please address correspondence to Matthew T. Whitehead, MD, Children's National Hospital, 111 Michigan Ave NW, Washington, DC, 20010; e-mail: MWhitehe@childrensnational.org

Indicates article with supplemental on-line table.

<http://dx.doi.org/10.3174/ajnr.A6446>

Multiple studies have shown that the MI may be small or absent more frequently in patients with schizophrenia spectrum disorders.^{2,10-15} It may also be small in borderline personality and bipolar disorders.^{16,17} MI abnormalities can also occur in association with Chiari II malformation, X-linked hydrocephalus, Cornelia de Lange syndrome, and diencephalic-mesencephalic junction dysplasia, among others.¹⁸⁻²²

The thalamic massa intermedia has never been formally evaluated in a group of exclusively pediatric patients, to our knowledge. We have observed that the MI is commonly absent, small, thickened, and/or displaced in patients with additional midline abnormalities. We sought to compare and contrast the prevalence, size, and location of the MI in 3T MR imaging examinations with normal findings in pediatric patients with and without congenital midline brain abnormalities and to determine whether there are structural variables that can predict MI abnormalities.

MATERIALS AND METHODS

After Children's National Hospital institutional review board approval, the MR imaging data base at a single academic pediatric hospital was searched for all consecutive 3T brain MR imaging examinations performed during 8 years (2012–2019) from pediatric patients (0–18 years of age) using the following key words/phrases: “normal brain,” “midline abnormality,” “agenesis,” “dysgenesis,” and “hypogenesis.” These terms were selected because they are a common lexicon used in neuroradiology reports from our institution to describe various midline malformations of the telencephalon, diencephalon, hindbrain, face, and skull. Each study was reviewed to verify the lack of abnormalities in the healthy group and the presence of ≥ 1 congenital midline abnormality in the abnormal group. Examinations with excessive motion artifacts, lack of 3D-T1WI, prior surgical intervention, tumor, and clastic lesions other than mild gliosis were excluded. In the healthy group, developmental delay and seizures were additional exclusion criteria. Age, sex, and examination indications were documented. Medical records were reviewed to clarify history and document diagnoses.

All MR imaging studies were performed on a 3T scanner (Signa HDxt Optima; GE Healthcare, Milwaukee, Wisconsin). Pulse sequences included a 3D sagittal echo-spoiled gradient-echo T1WI with 3 plane reformats, T2WI, T2-FLAIR, susceptibility-weighted (T2* weighted angiography), and DTI with 7 directions of encoding. 3D echo-spoiled gradient-echo T1WI parameters were the following: TE/TR = 3/8 ms, TI = 450 ms, flip angle = 12°, section thickness = 1 mm, section spacing = 0.5 mm, matrix = 256 × 256, FOV = 40–58 × 16–24 cm (based on head size). All examinations were evaluated, in consensus, by a board-certified neuroradiologist and pediatric neuroradiologist with 6 years of practice experience following certification (M.T.W.) and a second reader that had completed an Accreditation Council for Graduate Medical Education Pediatric Radiology Fellowship.

3D-T1WI was used to evaluate the MI presence, morphology (normal/thin/thick), location (third ventricle quadrant center),²³ anterior-posterior diameter, craniocaudal diameter, and surface area. The corpus callosum (presence, morphology, length, surface area, and diameters of the genu, rostrum, and splenium) and anterior commissure (presence, morphology, surface area, and

anterior-posterior and craniocaudal diameters) were assessed using sagittal 3D-T1WI. The transverse diameters of the MI, anterior commissure, and third ventricle were measured on reformatted axial 3D-T1WI. Additional brain structures were assessed qualitatively in the following manner: septum pellucidum (normal/cavum/hypoplastic/absent), fornix (normal/hypoplastic/absent), hypothalamus (normal/interhypothalamic adhesion), hippocampus (normal/under-rotated/dysplastic/sclerosis), vermis (normal/hypoplastic/dysplastic \pm hypoplastic), and brain stem (normal/hypoplastic/dysplastic \pm hypoplastic).

Using descriptive data derived from the healthy group, 2 SDs from the mean upper and lower bound cut points were determined for the MI, corpus callosum, and anterior commissure continuous data. Measurements falling below and above these boundaries were classified as “thin/hypoplastic” and “thickened/dysplastic,” respectively.

Statistical Methods

Normal Gaussian distribution of the data means was confirmed by a Shapiro-Wilk test. Subsequently, 2-tailed unpaired *t* tests were used to compare the continuous data means within and between the healthy and midline abnormality groups. χ^2 tests were used to evaluate categorical variable distribution differences within and between groups. Multiple logistic and linear regression analyses were conducted to determine whether there were age, sex, or MR imaging predictors of MI absence, size, or morphology. Additionally, logistic regression analyses were used to determine whether age predicted MI absence after controlling for sex. *P* < .05 was considered significant.

RESULTS

The healthy group comprised 111 examinations from 105 unique patients after excluding 4 cases (3D-T1WI lacking, *n* = 3; motion, *n* = 1). Six examinations from 5 patients were follow-ups. The most common primary indications were headache (*n* = 83) and encephalopathy (*n* = 11). The midline abnormality group consisted of 119 examinations from 103 patients after excluding 6 (catheters, *n* = 3; normal, *n* = 2; glioma, *n* = 1). Sixteen examinations from 14 patients were follow-ups. The most common primary indications in the abnormal group were fetal imaging with abnormal findings (*n* = 32), seizures (*n* = 16), dysmorphism (*n* = 15), and developmental delay (*n* = 10); a unifying diagnosis was achieved in 36/103 (35%), 19 (53%) of which were genetic diagnoses and 17 (47%) of which were clinical/imaging diagnoses, most commonly septo-optic dysplasia (*n* = 6) and Dandy-Walker malformation (*n* = 4). The average age of the healthy group was 11.7 \pm 5.3 years (range, 9 days to 18 years) versus 4.1 \pm 5.5 years (range, 1 day to 18 years) in the midline abnormality group (*P* < .001). There was no significant sex difference between groups (*P* = .78) (Table).

MI absence was more common in patients with midline abnormalities (41/103; 40%) than in patients with normal findings (13/105; 12%) (*P* < .001) (Figs 1–4). It was absent in 4/4 (100%) Dandy-Walker Malformation cases and 1/6 (17%) septo-optic dysplasia cases. The MI was duplicated in 1 case from the midline abnormality group. The MI transverse diameter was the only MI measurement with a statistical difference between

Demographic and structural variables in healthy and midline abnormality groups

| | Healthy Group (Avg \pm SD) | Midline Group (Avg \pm SD) | Total (Avg \pm SD) | P |
|-------------------------|--------------------------------|---|--|------|
| Age (yr) | 11.7 \pm 5.3 | 4.1 \pm 5.5 | 7.9 \pm 6.6 | .001 |
| Sex | n = 55 f (52%) | n = 52 f (50%) | n = 107 f (51%) | .78 |
| MI present | n = 92 (88%) | n = 62 (60%) | n = 154 (74%) | .001 |
| Morphology | n = 89 (n); 3(T) | n = 45 (n); 10(T); 7(t) | n = 134 (n); 13(T); 7(t) | .001 |
| tr (mm) | 1.5 \pm 0.2 | 2 \pm 0.2 | 1.7 \pm 1 | .002 |
| ap (mm) | 7.3 \pm 2.3 | 6.8 \pm 3.9 | 7 \pm 3.1 | .144 |
| cc (mm) | 6.7 \pm 5.6 | 6.1 \pm 3.5 | 6.4 \pm 4.9 | .202 |
| Area (mm ²) | 42.9 \pm 23.9 | 44.2 \pm 48.9 | 43.2 \pm 35.9 | .458 |
| Location | n = 84 (a/s); 6 (p/s); 2 (p/i) | n = 34 (a/s); 14 (p/s); 3 (p/i); 1 (a/i); 10 (all) | n = 118 (a/s); 20 (p/s); 5 (p/i); 1 (a/i); 10 (all) | .001 |
| CC present | n = 105 (100%) | n = 70 (68%) | n = 175 (84%) | .001 |
| Morphology | n = 105 (n) | n = 13 (n); 6 (h); 46 (h/d); 5 (d) | n = 118 (n); 6 (h); 46 (h/); (5d) | .001 |
| Length (mm) | 68.2 \pm 7.6 | 39.9 \pm 21.5 | 57 \pm 20.2 | .001 |
| Genu (mm) | 10.5 \pm 2 | 7.4 \pm 10 | 9.3 \pm 6.6 | .007 |
| Body (mm) | 5.7 \pm 1.2 | 3.5 \pm 2.2 | 4.9 \pm 1.9 | .001 |
| Splen (mm) | 10.3 \pm 2 | 4.7 \pm 2.9 | 8.4 \pm 3.6 | .001 |
| Area (mm ²) | 546 \pm 129 | 214 \pm 199 | 415 \pm 228 | .001 |
| AC present | n = 105 (100%) | n = 101 (98%) | n = 206 (99%) | .151 |
| Morphology | n = 105 (n) | n = 41 (n); 53 (h); 7 (T) | n = 146 (n); 53 (h); 7 (T) | .001 |
| tr (mm) | 1.8 \pm 0.4 | 3.9 \pm 1.5 | 2.8 \pm 1.5 | .001 |
| ap (mm) | 2.6 \pm 0.7 | 1.7 \pm 1.1 | 2.2 \pm 1 | .001 |
| cc (mm) | 3.5 \pm 1 | 2.2 \pm 1.3 | 2.9 \pm 1.3 | .001 |
| Area (mm ²) | 8.1 \pm 3.8 | 4.4 \pm 5.1 | 6.3 \pm 4.9 | .001 |
| Septum pellucidum | n = 96 (n); 9 (c) | n = 13 (n); 7 (c); 47 (a); 36 (h) | n = 109 (n); 16 (c); 47 (a); 36 (h) | .001 |
| Fornix | n = 105 (n) | n = 36 (n); 25 (a); 42 (h) | n = 141 (n); 25 (a); 42 (h) | .001 |
| Hypothalamus | n = 105 (n) | n = 84 (n); 19 (IHA) | n = 189 (n); 19 (IHA) | .001 |
| Hippocampus | n = 87 (n); 18 (u) | n = 11 (n); 88 (u); 2 (d); 2 (mts) | n = 98 (n); 106 (u); 2 (d); 2 (mts) | .001 |
| Brain stem | n = 105 (n) | n = 67 (n); 18 (h); 18 (d) | n = 172 (n); 18 (h); 18 (d) | .001 |
| Vermis | n = 105 (n) | n = 77 (n); 15 (h); 11 (d) | n = 182 (n); 15 (h); 11 (d) | .001 |
| 3rd Ventricle (mm) | 2.8 \pm 0.9 | 5.5 \pm 3.3 | 4.1 \pm 2.8 | .001 |

Note:—Avg indicates average; tr, transverse diameter; ap, anteroposterior diameter; cc, craniocaudal diameter; CC, corpus callosum; Splen, splenium; AC, anterior commissure; n, normal; T, thick; t, thin; a/s, anterior/superior quadrant of 3rd ventricle; a/i, anterior-inferior; p/s, posterior-superior; p/i, posterior-inferior; all, all quadrants; h, hypoplastic; h/d, hypogenetic \pm dysgenetic; d, dysgenetic/dysplastic; c, cavum; a, absent; IHA, interhypothalamic adhesion; u, under-rotated; mts, hippocampal sclerosis; f, female.

groups. The MI mean surface area was not significantly different between groups (healthy group, 43 ± 24 mm; range, 6–140 mm; abnormal group, 44 ± 49 mm; range, 2–214 mm; $P = .46$). However, the MI morphology differed and was almost always normal in examinations with normal findings (89/92, 97%) and frequently-but-less commonly normal in patients with midline abnormalities (45/62, 73%) ($P < .001$) (Figs 5 and 6). Furthermore, the MI location differed between groups; in examinations with normal findings, it was almost always centered in the anterior/superior quadrant of the third ventricle ($n = 84$, 91%) and was more variable in patients with midline abnormalities ($P < .001$). Neither MI presence nor surface area nor morphology was predictable on the basis of age or sex ($P > .05$). There was no significant change in the presence, size, morphology, or location of the MI on any of the 6 follow-up examinations in the healthy group; however, 6/11 (55%) follow-up examinations from patients with an MI in the abnormal group had interval MI volume loss. When the MI surface area remained stable on follow-up, there was no significant change in third ventricle diameter in either group ($P > .67$). However, the third ventricle diameter significantly increased when the MI surface area decreased ($P = .013$). Specific data of additional groups are presented in the Table.

Logistic regression analysis showed that the odds of an absent MI were 1.5 times greater (OR, 0.68; 95% CI, 0.59–0.79; $P < .001$)

with every 1-mm increase in the third ventricle transverse diameter and 1.7 times greater (OR, 0.6; 95% CI, 0.48–0.75; $P < .001$) with every 1-mm increase in the anterior commissure transverse diameter in both groups combined. Furthermore, third ventricle diameter and anterior commissure diameter were strong predictors of MI surface area and morphology in both groups combined ($P < .001$). Corpus callosum presence was predictive of MI presence (OR, 3.9; 95% CI, 1.8–8.5; $P < .001$) and MI area ($P = .002$) in both groups combined. Interhypothalamic adhesions were predictive of MI surface area and morphology in both groups combined ($P < .03$). Hippocampal abnormalities tripled the odds of MI absence (OR, 0.33; 95% CI, 0.17–0.65; $P < .001$) and were predictive of MI surface area and morphology abnormalities ($P < .02$) in both groups combined. Brain stem hypoplasia or dysplasia or both were predictive of MI surface area and morphology in both groups combined ($P < .001$). The odds of MI absence were 2.4 times greater in patients with vermian hypoplasia and/or dysplasia (OR, 0.42; 95% CI, 0.24–0.73; $P = .002$) in both groups combined (On-line Table).

DISCUSSION

The thalamic massa intermedia is more commonly absent (40% versus 12%), dysmorphic, and/or displaced in children with other structural midline brain abnormalities than in those without. MI

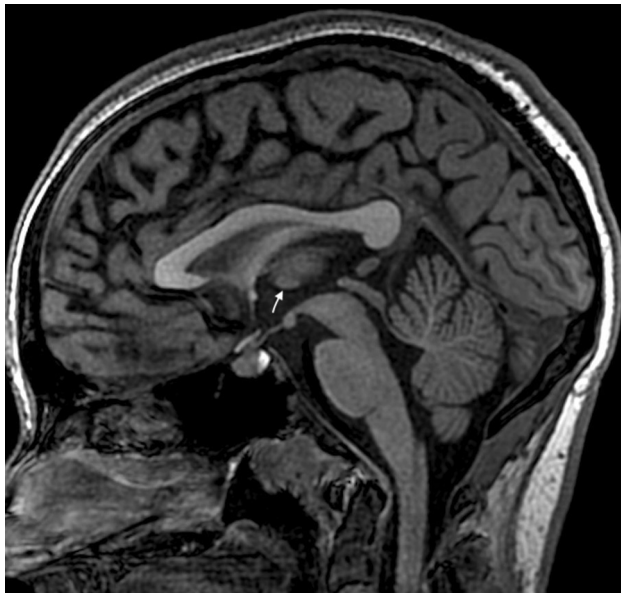


FIG 1. Sagittal midline T1WI from a brain MR imaging with normal findings in a 17-year-old adolescent girl with retroauricular pain depicting the normal thalamic MI centered in the anterior/superior portion of the third ventricle (*arrow*).

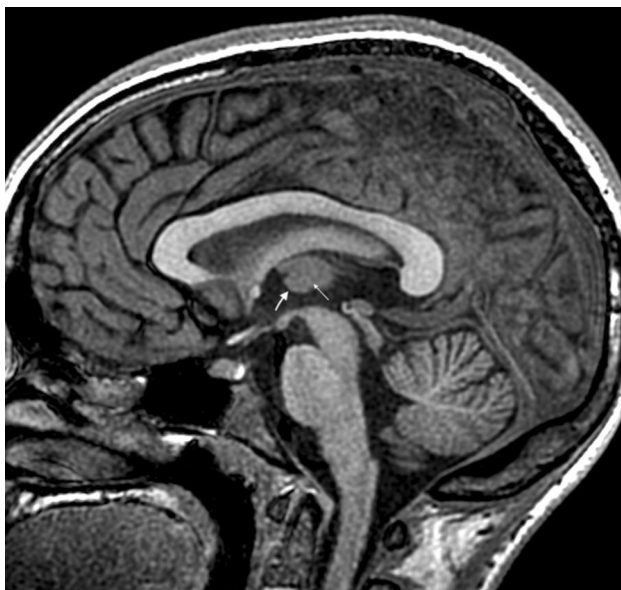


FIG 2. Sagittal midline T1WI from a brain MR imaging with normal findings in an 11-year-old girl with headache, showing a normal MI with part of its superior and posterior margin volume averaged with the medial thalami in a patient with a small third ventricle (*large arrow*). This appearance has the potential to compromise MI evaluation both qualitatively and quantitatively. However, a faint marginal distinction is often seen when carefully analyzed (*small arrow*).

absence, surface area, and morphology are predictable by various attributes and abnormalities involving the corpus callosum, anterior commissure, hippocampus, hypothalamus, vermis, brain stem, and third ventricle.

Midline brain malformations are often multiple and may involve the MI. For example, the MI diameter is generally smaller



FIG 3. Sagittal midline T1WI demonstrating MI absence in association with multiple additional midline abnormalities, including marked enlargement of the fourth ventricle/posterior fossa and under-rotation of a hypoplastic/dysplastic vermis (Dandy-Walker malformation), hypoplasia of the anterior commissure (*arrow*), pontine hypoplasia, and agenesis of the corpus callosum.

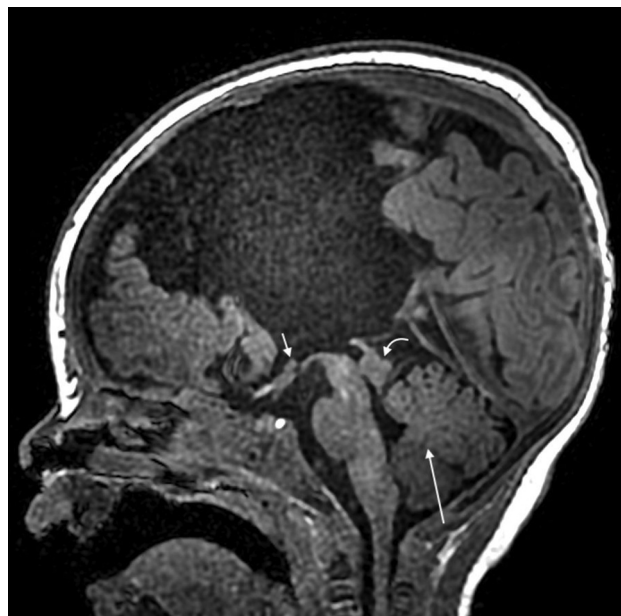


FIG 4. Sagittal midline T1WI showing MI absence in association with multiple additional midline abnormalities in a patient with septo-optic holoprosencephaly. Additional findings include agenesis of the corpus callosum, interhypothalamic adhesion (*small straight arrow*), tectal dysplasia (*small curved arrow*), and hypoplasia of the vermis (*long straight arrow*).

in fetuses with corpus callosum agenesis.²⁴ In our experience, the MI is an often-neglected midline brain component on MR imaging, perhaps due to lack of familiarity/awareness, perceived lack of importance, and/or satisfaction with the search when other

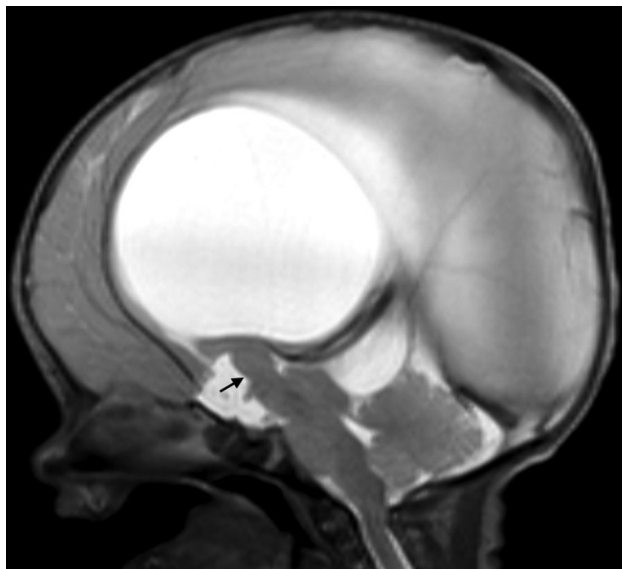


FIG 5. Sagittal midline T2WI from a patient with diencephalic-mesencephalic junction dysplasia showing a thickened thalamic massa intermedia connected to the midbrain (arrow). The midbrain is dysplastic with associated aqueductal stenosis and consequent hydrocephalus.

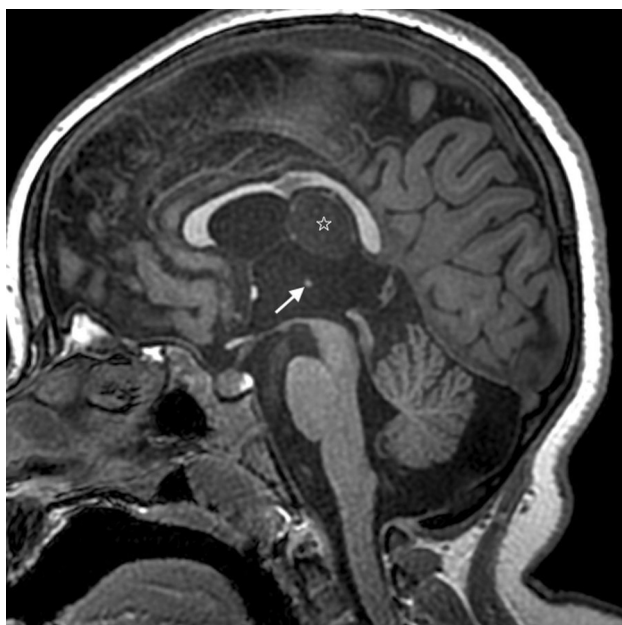


FIG 6. Sagittal midline T1WI depicting MI thinning/hypoplasia in a patient with Aicardi syndrome (arrow). Other findings include callosal dysgenesis and a pericallosal arachnoid cyst (star).

abnormalities exist. However, 1 midline abnormality should heighten radiologists' suspicion for others, and all abnormalities should be carefully documented in an effort to diagnose an underlying syndrome/disorder, or at least to lay the groundwork for a future diagnosis. Massa intermedia abnormalities can be a clue to the presence of additional abnormalities.

The MI mean surface area was $43 \pm 24 \text{ mm}^2$ in examinations with normal findings. This is congruent with previous pathology literature comprising mostly adult specimens (mean surface area range, $13\text{--}46 \text{ mm}^2$).^{25–28} Although the average MI surface area

did not significantly differ between groups, MI dysmorphology was more common in the midline abnormality group (27% versus 3%). MI dysmorphology has been reported in several diseases. Chiari II malformation-related MI thickening may be the best-known disease-associated condition.¹⁸ Yamasaki et al¹⁹ found MI thickening in all 6 patients with X-linked hydrocephalus examined by MR imaging. Loss of function *L1 cell adhesion molecule (LICAM)* gene defects seems to result in the most severe neuroimaging phenotype, with 100% prevalence of MI thickening.²⁰ In diencephalic-mesencephalic junction dysplasia, the MI may be dysplastic and connected to the midbrain.²² MI thickening was also demonstrated in 60% (3/5) of patients with 6q terminal deletion syndrome.²⁹

MI size tends to decrease with age in adults.^{15,25,30} However, the association between MI abnormality and age has not been previously addressed in children. We found no relationship between age and MI abnormalities. On the other hand, the MI surface area decreased in more than one-third of follow-up examinations in the midline abnormality group. The transverse diameters of the MI, anterior commissure, and third ventricle were correlated variables, and the MI area was inversely related to them. Prior studies have also shown inverse relationships between the third ventricle diameter and MI thickness.^{3,10,24,30,31} Acquired MI absence can occur secondary to hydrocephalus-induced rupture.³² If we add our findings to the existing literature, it seems that MI volume loss and/or absence can occur in 3 main scenarios: 1) congenital, decreased or lack of the normal MI constraint leading to third ventriculomegaly; 2) acquired, primary or secondary MI volume loss associated with loss of cerebral volume; and 3) acquired, increased third ventricular pressure/dilation causing stretching or rupture.

MI duplication has been sparsely described on postmortem examination and imaging.^{26,28,33–35} By means of MR imaging, it has been shown in Dandy-Walker continuum and in a patient with a presumed-but-unknown genetic disorder.^{33,34} The MI was duplicated in 1 of our patients with midline malformations, including callosal dysgenesis and anterior commissure hypoplasia.

Previous literature mainly from adult subjects has shown the prevalence of MI absence in healthy subjects to be 2%–25%; this wide range is probably related to varied imaging and pathology techniques used in its assessment.^{2,3,5,11–13,15,25–28,31,36} Two prior imaging studies, one primarily and the other exclusively in adults, performed using 3T MR imaging and 1-mm-thick sections akin to our study, found the normal prevalence of MI absence to be 4%–10%.³⁵ Similar to these, we discovered MI absence in 12% of pediatric patients with otherwise normal MR imaging findings. MI absence may be present at a higher rate in association with other brain malformations. For instance, the MI was absent in greater than one-third of patients with Cornelia de Lange syndrome in 1 study.²¹ We determined that the MI was more likely to be absent in children with additional structural midline brain abnormalities. Furthermore, the MI was absent in all of our patients with Dandy-Walker malformation and infrequently in septo-optic dysplasia.

Reported MI sex differences have been conflicting, but many studies have suggested a higher prevalence of MI absence and decreased MI volume in males compared with

females.^{5,23,27,28,31,36} In contrast, we found no significant sex differences between groups among the variables examined. It is possible that the reported sexual dimorphism of the MI may be present only in the adult population.

MI location impacts local CSF flow dynamics.²³ The maximum pressure within the third ventricle can vary up to 50% on the basis of MI location.²³ In healthy patients, the MI tends to be centered in the anterior/superior quadrant of the third ventricle.^{26,28} Our findings are in agreement. However, it was significantly more variable in location in the midline abnormality group.

Hippocampal abnormalities increased the likelihood of MI absence, altered surface area, and abnormal morphology. Animal studies have demonstrated functional connectivity between the medial temporal lobes and MI. In felines with amygdaloid-stimulation-induced seizure kindling, the MI plays a role in interhemispheric ictal propagation.³⁷ MI-induced kindling in rats resembles an amygdaloid kindling response.³⁸ N-methyl-D-aspartate injection into the MI induces seizures and facilitates limbic kindling in rats.^{39,40} However, under-rotation, or “incomplete hippocampal inversion” may be found in up to 17% of healthy subjects, similar to our findings in the brain MR imaging group with normal findings.⁴¹

MI absence, surface area, and morphology were predicted by the presence of an interhypothalamic adhesion. Congenital interhypothalamic adhesions may be markers of additional midline abnormalities.⁴²⁻⁴⁵

Several limitations warrant mention. We acknowledge that MI prevalence and size cannot be verified without histologic correlation. However, 3-plane high-resolution T1WIs were carefully scrutinized to make determinations. Furthermore, MI prevalence and size in the healthy group are within the range previously reported for healthy adults. Even with current state-of-the-art MR imaging techniques, however, MI absence may be underappreciated because volume averaging remains a challenge, especially when the third ventricle is small (Fig 2). Therefore, there is a tendency to underdiagnose MI absence and overestimate MI size with neuroimaging. Another limitation is that the mean age between groups was statistically different, with the abnormal group being imaged at a younger age on average. This difference was unavoidable given the retrospective nature of the study. Nonetheless, there was no difference within or between groups with regard to MI absence, area, or morphology. Another potential limitation is that most patients in the healthy group were imaged due to headache symptoms, making pediatric migraine a potential-albeit-unlikely confounding variable. Finally, few unified diagnoses were known in the midline abnormality group, limiting disease-specific generalizability. Future work would be useful to determine whether disease-specific MI abnormalities exist.

CONCLUSIONS

Most pediatric patients have a thalamic massa intermedia centered in the anterior/superior third ventricle. The MI is more frequently absent, dysmorphic, and/or displaced in pediatric patients with additional midline abnormalities than in those

without. These findings support the notion that the MI cannot be ignored during MR imaging assessment of the brain. It can be a clue to the presence of additional abnormalities. Normal-variant MI absence is a diagnosis of exclusion, which should only be proposed when it is isolated and in patients without any associated clinical deficits.

REFERENCES

- O’Rahilly R, Müller F. **Ventricular system and choroid plexuses of the human brain during the embryonic period proper.** *Am J Anat* 1990;189:285–302 [CrossRef Medline](#)
- Trzesniak C, Linares IM, Coimbra ÉR, et al. **Adhesio interthalamica and cavum septum pellucidum in mesial temporal lobe epilepsy.** *Brain Imaging Behav* 2016;10:849–56 [CrossRef Medline](#)
- Yasaka K, Akai H, Kunimatsu A, et al. **Factors associated with the size of the adhesio interthalamica based on 3.0-T magnetic resonance images.** *Acta Radiol* 2019;60:113–19 [CrossRef Medline](#)
- Laslo P, Slobodan M, Nela P, et al. **Specific circular organization of the neurons of human interthalamic adhesion and of periventricular thalamic region.** *Int J Neurosci* 2005;115:669–79 [CrossRef Medline](#)
- Damle NR, Ikuta T, John M, et al. **Relationship among interthalamic adhesion size, thalamic anatomy and neuropsychological functions in healthy volunteers.** *Brain Struct Funct* 2017;222:2183–92 [CrossRef Medline](#)
- Kochanski RB, Dawe R, Kocak M, et al. **Identification of stria medullaris fibers in the massa intermedia using diffusion tensor imaging.** *World Neurosurg* 2018;112:e497–504 [CrossRef Medline](#)
- Molinari M, Minciacci D, Bentivoglio M, et al. **Efferent fibers from the motor cortex terminate bilaterally in the thalamus of rats and cats.** *Exp Brain Res* 1985;57:305–12 [CrossRef Medline](#)
- Pritzel M, Sarter M, Morgan S, et al. **Interhemispheric nigrostriatal projections in the rat: bifurcating nigral projections and loci of crossing in the diencephalon.** *Brain Res Bull* 1983;10:385–90 [CrossRef Medline](#)
- Lumley JS. **The role of the massa intermedia in motor performance in the rhesus monkey.** *Brain* 1972;95:347–56 [CrossRef Medline](#)
- Snyder PJ, Bogerts B, Wu H, et al. **Absence of the adhesio interthalamica as a marker of early developmental neuropathology in schizophrenia: an MRI and postmortem histologic study.** *J Neuroimaging* 1998;8:159–63 [CrossRef Medline](#)
- Takahashi T, Suzuki M, Zhou SY, et al. **Prevalence and length of the adhesio interthalamica in schizophrenia spectrum disorders.** *Psychiatry Res* 2008;164:90–94 [CrossRef Medline](#)
- Ceyhan M, Adapinar B, Aksaray G, et al. **Absence and size of massa intermedia in patients with schizophrenia and bipolar disorder.** *Acta Neuropsychiatr* 2008;20:193–98 [CrossRef Medline](#)
- Trzesniak C, Kempton MJ, Busatto GF, et al. **Adhesio interthalamica alterations in schizophrenia spectrum disorders: a systematic review and meta-analysis.** *Prog Neuropsychopharmacol Biol Psychiatry* 2011;35:877–86 [CrossRef Medline](#)
- Trzesniak C, Schaufelberger MS, Duran FL, et al. **Longitudinal follow-up of cavum septum pellucidum and adhesio interthalamica alterations in first-episode psychosis: a population-based MRI study.** *Psychol Med* 2012;42:2523–34 [CrossRef Medline](#)
- Takahashi T, Nakamura K, Ikeda E, et al. **Longitudinal MRI study of the midline brain regions in first-episode schizophrenia.** *Psychiatry Res* 2013;212:150–53 [CrossRef Medline](#)
- Takahashi T, Malhi GS, Wood SJ, et al. **Midline brain abnormalities in established bipolar affective disorder.** *J Affect Disord* 2010;122:301–05 [CrossRef Medline](#)
- Takahashi T, Chanen AM, Wood SJ, et al. **Midline brain structures in teenagers with first-presentation borderline personality disorder.** *Prog Neuropsychopharmacol Biol Psychiatry* 2009;33:842–46 [CrossRef Medline](#)

18. Etus V, Guler TM, Karabagli H. **Third ventricle floor variations and abnormalities in myelomeningocele-associated hydrocephalus: our experience with 455 endoscopic third ventriculostomy procedures.** *Turk Neurosurg* 2017;27:768–71 [CrossRef Medline](#)
19. Yamasaki M, Arita N, Hiraga S, et al. **A clinical and neuroradiological study of X-linked hydrocephalus in Japan.** *J Neurosurg* 1995;83:50–55 [CrossRef Medline](#)
20. Kanemura Y, Okamoto N, Sakamoto H, et al. **Molecular mechanisms and neuroimaging criteria for severe L1 syndrome with X-linked hydrocephalus.** *J Neurosurg* 2006;105:403–12 [CrossRef Medline](#)
21. Whitehead MT, Nagaraj UD, Pearl PL. **Neuroimaging features of Cornelia de Lange syndrome.** *Pediatr Radiol* 2015;45:1198–205 [CrossRef Medline](#)
22. Severino M, Tortora D, Pistorio A, et al. **Expanding the spectrum of congenital anomalies of the diencephalic-mesencephalic junction.** *Neuroradiology* 2016;58:33–44 [CrossRef Medline](#)
23. Cheng S, Tan K, Bilston LE. **The effects of the interthalamic adhesion position on cerebrospinal fluid dynamics in the cerebral ventricles.** *J Biomech* 2010;43:579–82 [CrossRef Medline](#)
24. Birnbaum R, Parodi S, Donarini G, et al. **The third ventricle of the human fetal brain: normative data and pathologic correlation: a 3D transvaginal neurosonography study.** *Prenat Diagn* 2018;38:664–72 [CrossRef Medline](#)
25. Davie JC, Baldwin M. **Radiographic-anatomical study of the massa intermedia.** *J Neurosurg* 1967;26:483–87 [CrossRef Medline](#)
26. Malobabić S, Puskas L, Blagotić M. **Size and position of the human adhaesio interthalamica.** *Gegenbaurs Morphol Jahrb* 1997;133:175–80 [Medline](#)
27. Allen LS, Gorski RA. **Sexual dimorphism of the anterior commissure and massa intermedia of the human brain.** *J Comp Neurol* 1991;312:97–104 [CrossRef Medline](#)
28. Pavlović MN, Jovanović ID, Ugrenović SZ, et al. **Position and size of massa intermedia in Serbian brains.** *Folia Morphol (Warsz)* 2019 Apr 17. [CrossRef Medline](#)
29. Elia M, Striano P, Fichera M, et al. **6q terminal deletion syndrome associated with a distinctive EEG and clinical pattern: a report of five cases.** *Epilepsia* 2006;47:830–38 [CrossRef Medline](#)
30. Rosales RK, Lemay MJ, Yakovlev PI. **The development and involution of massa intermedia with regard to age and sex.** *J Neuropathol Exp Neurol* 1968;27:166 [Medline](#)
31. Samra KA, Cooper IS. **Radiology of the massa intermedia.** *Radiology* 1968;91:1124–28 [CrossRef Medline](#)
32. El Damaty A, Langner S, Schroeder HW. **Ruptured massa intermedia secondary to hydrocephalus.** *World Neurosurg* 2017;97:749.e7–10 [CrossRef Medline](#)
33. Tubbs RS, Smyth MD, Oakes WJ, et al. **Duplication of the massa intermedia in a child.** *Pediatr Neurosurg* 2004;40:42–43 [CrossRef Medline](#)
34. Whitehead MT. **Thalamic massa intermedia duplication in a dysmorphic 14 month-old toddler.** *J Radiol Case Rep* 2015;9:1–5 [CrossRef Medline](#)
35. Baydin S, Gungor A, Baran O, et al. **The double massa intermedia.** *Surg Neurol Int* 2016;7:30 [CrossRef Medline](#)
36. Nopoulos PC, Rideout D, Crespo-Facorro B, et al. **Sex differences in the absence of massa intermedia in patients with schizophrenia versus healthy controls.** *Schizophr Res* 2001;48:177–85 [CrossRef Medline](#)
37. Hiyoshi T, Wada JA. **Midline thalamic lesion and feline amygdaloid kindling, I: effect of lesion placement prior to kindling.** *Electroencephalogr Clin Neurophysiol* 1988;70:325–38 [CrossRef Medline](#)
38. Mori N, Wada JA. **Kindling of the massa intermedia of the thalamus in rats.** *Brain Res* 1992;575:148–50 [CrossRef Medline](#)
39. Hirayasu Y, Wada JA. **N-methyl-D-aspartate injection into the massa intermedia facilitates development of limbic kindling in rats.** *Epilepsia* 1992;33:965–70 [CrossRef Medline](#)
40. Hirayasu Y, Wada JA. **Convulsive seizures in rats induced by N-methyl-D-aspartate injection into the massa intermedia.** *Brain Res* 1992;577:36–40 [CrossRef Medline](#)
41. Cury C, Toro R, Cohen F, et al; IMAGEN Consortium. **Incomplete hippocampal inversion: a comprehensive MRI study of over 2000 subjects.** *Front Neuroanat* 2015;9:160 [CrossRef Medline](#)
42. Whitehead MT, Vezina G. **Interhypothalamic adhesion: a series of 13 cases.** *AJNR Am J Neuroradiol* 2014;35:2002–06 [CrossRef Medline](#)
43. Ahmed FN, Stence NV, Mirsky DM. **Asymptomatic interhypothalamic adhesions in children.** *AJNR Am J Neuroradiol* 2016;37:726–29 [CrossRef Medline](#)
44. Whitehead MT, Vezina G. **Asymptomatic interhypothalamic adhesions in children.** *AJNR Am J Neuroradiol* 2016;37:E35 [CrossRef Medline](#)
45. Loubet A, Dargazanli C, Joris Roux C, et al. **Interhypothalamic adhesion and multiple cerebral abnormalities in a 2-year-old boy.** *J Neuroradiol* 2017;44:63–64 [CrossRef Medline](#)